

Observation of Symmetry-Protected Dirac States in Nonsymmorphic α -Antimonene

Qiangsheng Lu,¹ Kyle Y. Chen,² Matthew Snyder,¹
Jacob Cook,¹ Duy Tung Nguyen,¹ and Guang Bian¹

¹*Department of Physics and Astronomy,
University of Missouri, Columbia, Missouri 65211, USA*
²*Rock Bridge High School, Columbia, Missouri 65203, USA*

(Dated: December 23, 2024)

Abstract

The discovery of graphene has stimulated enormous interest in two-dimensional (2D) electron gas with linear band dispersion. However, to date, 2D Dirac semimetals are still very rare due to the fact that 2D Dirac states are generally fragile against perturbations such as spin-orbit couplings. Nonsymmorphic crystal symmetries can enforce the formation of Dirac nodes, providing a new route to establishing symmetry-protected Dirac states in 2D materials. Here we report the symmetry-protected Dirac states in nonsymmorphic α -antimonene (Sb monolayer). The antimonene was synthesized by the method of molecular beam epitaxy. Two Dirac cones with large anisotropy were observed by angle-resolved photoemission spectroscopy. The Dirac states in α -antimonene is of spin-orbit type in contrast to the spinless Dirac states in graphene. The result extends the “graphene” physics into a new family of 2D materials where spin-orbit coupling is present.

Dirac states with linear band dispersion and vanishing effective mass have been discovered in condensed matter materials such as graphene, topological insulators, and bulk Dirac semimetals. [1–3]. The topological phase of Dirac fermion states leads to many exotic physical properties such as zero-energy Landau levels [4]. The graphene-like Dirac materials have been considered as a cornerstone for the development of next-generation electronic devices. However, the two-dimensional Dirac cones are generally unstable because an energy gap can be easily induced by intrinsic or extrinsic perturbations such as spin-orbit coupling (SOC) and lattice distortions. This leads to the rarity of 2D Dirac materials, and only a few materials have been proved experimentally to host gapless 2D Dirac states, including graphene [1, 2] and the surface of topological insulators [3]. The Dirac states in graphene can be considered to be gapless only by ignoring the small SOC of the system. When the dimension of topological insulators is reduced, a tunneling energy gap opens at the Dirac point, which is due to the hybridization of the surface states on the opposite surfaces [3]. To realize exactly gapless Dirac states, geometrical constraints on the crystal lattice are generally needed to protect the nodal points against various gapping mechanisms.

Recently, it has been proposed that nonsymmorphic crystalline symmetries including glide mirrors and screw axes can enforce band crossings and hence induce Dirac-fermion like states [5–9]. This is because the operator of nonsymmorphic symmetry operations create only high-dimensional irreducible representations at certain symmetry points of the Brillouin zone [7, 9]. This presents a new route to realizing 2D Dirac materials whose Dirac states are robust even in the presence of strong SOC. Here we report the observation of 2D Dirac states in the α -phase of antimonene (monolayer antimony). Bulk Sb is a group-V semimetal with a small overlap between the valence and conduction bands. Despite small electron and hole pockets at the Fermi level, there exists an indirect negative energy gap traversing the whole Brillouin zone and separating the valence and conduction bands [10]. This gapped band structure enables Sb, though semimetallic, to host the same \mathbf{Z}_2 topological invariants as topological insulators [3]. The large spin-orbit coupling plays the key role in the generation of the nontrivial band topology. In the 2D limit, monolayer Sb, *i.e.*, antimonene, are known to have two allotropic structural phases, namely, the black-phosphorus (BP)-like α -phase and the hexagonal β -phase. The lattice of α -antimonene (α -Sb for short) is nonsymmorphic, therefore α -Sb can host symmetry-protected Dirac states. In this work, we synthesized α -Sb by the technique of molecular beam epitaxy (MBE) and detected the 2D Dirac states by

angle-resolved photoemission (ARPES) experiments. The results shed light to the search of 2D Dirac materials in the vast territory of 2D nonsymmorphic crystals.

EXPERIMENTAL RESULTS

In our experiment, α -Sb was grown on SnSe substrates under an ultrahigh vacuum environment. The SnSe crystals was cleaved *in situ* and provided an atomically flat surface for the deposition of Sb. The crystallographic structure of α -Sb is schematically shown in Figs 1(a) and 1(b). The surface unit cell is marked by a blue rectangular box. The in-plane lattice constants are 4.49 and 4.30 Å. The in-plane nearest-neighbor bond length is 2.90 Å. α -Sb consists of two horizontal atomic sublayers. Each atomic sublayer is perfectly flat according to first-principles lattice relaxations. For a single layer (1L) of α -Sb, the vertical spacing between the two atomic sublayers is 2.79 Å. For a two-layer (2L) α -Sb film, the vertical distance between the two atomic sublayers within each α -Sb layer is 2.89 Å while the spacing between the two layers of α -Sb is 3.18 Å. The structure of one- and two-layer α -Sb belongs to the #42 layer group (*pman*). The lattice is invariant under a glide mirror reflection operation. The glide mirror is parallel to the x - y planes, and lies in the middle between the two atomic sublayers of 1L α -Sb. The glide mirror reflection is composed of a mirror reflection and an in-plane translation by $(0.5a, 0.5b)$. For 2L α -Sb, the glide mirror sits in the middle between the two α -Sb layers. Figures 1(c-e) show the STM image of two Sb/SnSe samples with atomic resolution. The first sample consists of mainly 1L α -Sb islands, see Fig. 1(c). A line-mode reconstruction (Moiré pattern) can be seen on the α -Sb surface, as marked by the green dashed lines. The height profile taken along the the blue arrow (shown in Fig. 1(d)) indicates that the height of the 1L α -Sb island is 6.5 Å. The second sample possesses both 1L and 2L domains as shown in Fig. 1(e).

The glide mirror symmetry of the lattice leads to band degeneracy at high-symmetry points \bar{X}_1 and \bar{X}_2 . The Brillouin zone of α -Sb is plotted in Fig. 2(a). We performed first-principles calculations for 1L and 2L α -Sb films. The results are shown in Figs. 2(b) and 2(c). Both 1L and 2L α -Sb have a semiconducting electronic structure, which can be seen in the calculated density of states. Apparently, there exist band crossings at points \bar{X}_1 and \bar{X}_2 . The band degeneracy occurs for every band at these two high-symmetry points. Each band splits into two branches as it disperses away from $\bar{X}_{1,2}$. Therefore, the band crossings

at $\bar{X}_{1,2}$ create 2D Dirac states. The Dirac points at \bar{X}_1 and \bar{X}_2 in the top valence band are marked by "D1" and "D2", respectively. We note that the location of Dirac points is entirely determined by the underlying nonsymmorphic lattice symmetry [11].

The ARPES result taken from the 1L α -Sb sample is shown in Fig. 3. There are three prominent features on the Fermi surface, namely, one electron pocket at $\bar{\gamma}$ and two hole pocket near \bar{X}_2 , see Fig. 3(a). The band spectrum take along \bar{X}_2 - $\bar{\Gamma}$ - \bar{X}_2 and \bar{X}_1 - $\bar{\Gamma}$ - \bar{X}_1 directions are plotted in Figs 3(b) and 3(c). The calculated band dispersion is overlaid on the ARPES spectrum for a comparison. The theoretical bands agree with the ARPES spectrum, especially both showing the band crossings at \bar{X}_1 and \bar{X}_2 . Figures 3(d) and 3(e) show the band dispersion around \bar{X}_1 and \bar{X}_2 in a perpendicular direction. In the \bar{M} - \bar{X}_2 - \bar{M} direction, the two subbands dispersing a way from the Dirac nodes are nearly degenerate, which leads to a huge anisotropy in the Dirac band contours. The anisotropy of Dirac bands is less prominent in the \bar{M} - \bar{X}_1 - \bar{M} direction. We note that the minor discrepancy between the ARPES spectrum and first-principles bands can be attributed to the substrate effects in the MBE samples. The ARPES results taken from the 2L α -Sb sample is shown in Fig.4. According to the STM characterization, the sample possesses 1L and 2L domains, therefore we can see contributions of 1L and 2L to the total ARPES spectrum. From a comparison with the calculated bands, we can identify the spectrum from 2L α -Sb films. The ARPES results again show Dirac points (band degeneracy) at \bar{X}_1 and \bar{X}_2 . The Dirac cone centered at \bar{X}_2 exhibits a large anisotropy in the band dispersion. The ARPES results together with the first-principles band simulations unambiguously demonstrate the existence of 2D Dirac states in the nonsymmorphic α -Sb films.

CONCLUSION

Our ARPES measurements and first-principles calculations showed that α -Sb hosts Dirac-fermion states at the high-symmetry momentum points \bar{X}_1 and \bar{X}_2 . The band degeneracy at the Dirac points are strictly protected by the nonsymmorphic symmetry of the lattice. The lattice symmetry guarantees that the Dirac states in α -Sb are robust even in the presence of strong SOC. Actually, the SOC plays an important role in the formation of Dirac states. Without SOC, the two branches of the Dirac cone become degenerate along $\bar{X}_{1,2} - \bar{M}$ directions and result in a nodal-line band structure [11]. In this sense, the Dirac states of α -Sb

are spin-orbit coupled, in contrast to the spinless ones of graphene. Breaking the lattice symmetry, on the other hand, can lift the band degeneracy at Dirac points and yield gapped phases [11]. This correspondence principle of lattice symmetry and nodal band structure applies to all 2D nonsymmorphic crystalline materials. The results open a door for exploring novel "graphene" physics in a rich material pool of nonsymmorphic materials.

-
- [1] K. S. Novoselov, A. K. Geim, S. V. Morozov, D. Jiang, M. I. Katsnelson, I. V. Grigorieva, S. V. Dubonos, and A. A. Firsov, *Nature* **438**, 197 (2005), ISSN 0028-0836.
 - [2] Y. Zhang, Y.-W. Tan, H. L. Stormer, and P. Kim, *Nature* **438**, 201 (2005).
 - [3] M. Z. Hasan and C. L. Kane, *Rev. Mod. Phys.* **82**, 3045 (2010).
 - [4] A. H. Castro Neto, F. Guinea, N. M. R. Peres, K. S. Novoselov, and A. K. Geim, *Rev. Mod. Phys.* **81**, 109 (2009).
 - [5] S. M. Young and C. L. Kane, *Phys. Rev. Lett.* **115**, 126803 (2015).
 - [6] S. Guan, Y. Liu, Z.-M. Yu, S.-S. Wang, Y. Yao, and S. A. Yang, *Phys. Rev. Mater.* **1**, 054003 (2017).
 - [7] B. J. Wieder and C. L. Kane, *Phys. Rev. B* **94**, 155108 (2016).
 - [8] B. J. Wieder, B. Bradlyn, Z. Wang, J. Cano, Y. Kim, H.-S. D. Kim, A. M. Rappe, C. L. Kane, and B. A. Bernevig, *Science* **361**, 246 (2018).
 - [9] H. C. Po, A. Vishwanath, and H. Watanabe, *Nat. Commun.* **8**, 50 (2017), ISSN 2041-1723.
 - [10] Y. Liu and R. E. Allen, *Phys. Rev. B* **52**, 1566 (1995), URL <https://link.aps.org/doi/10.1103/PhysRevB.52.1566>.
 - [11] P. J. Kowalczyk, S. A. Brown, T. Maerkl, Q. Lu, C.-K. Chiu, Y. Liu, S. A. Yang, X. Wang, I. Zasada, F. Genuzio, et al., *ACS Nano* **14**, 1888 (2020), ISSN 1936-0851, URL <https://doi.org/10.1021/acsnano.9b08136>.

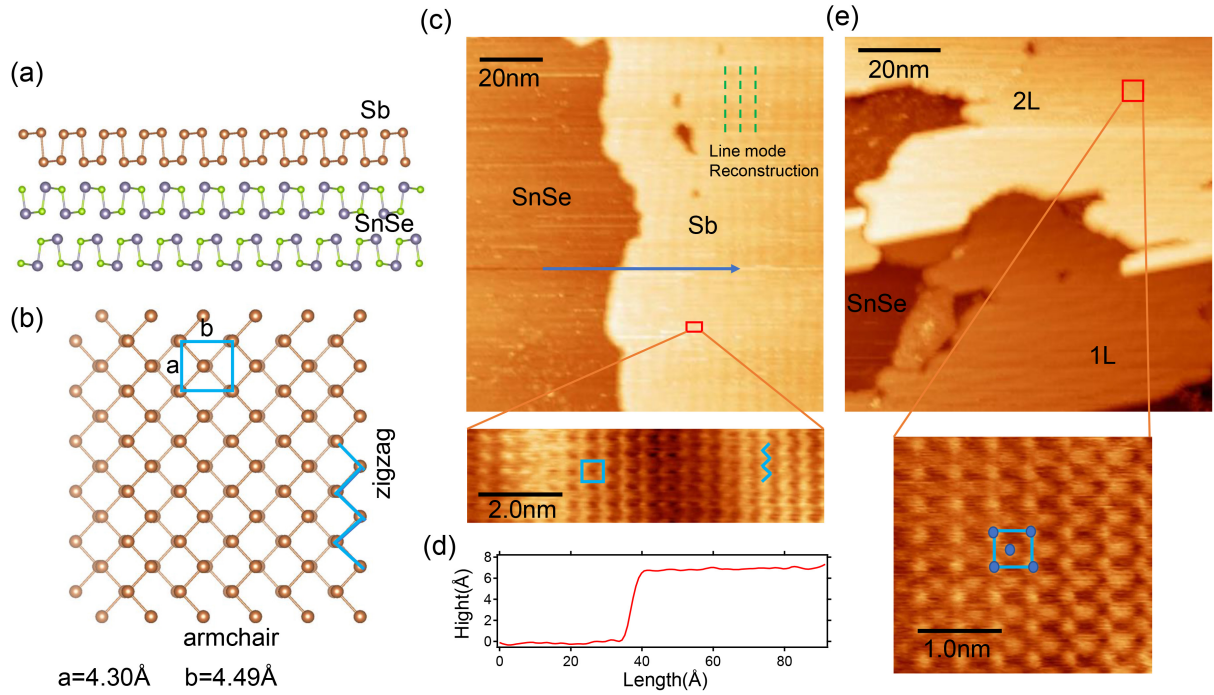


FIG. 1: (a) Side view of α -Sb/SnSe lattice structure. (b) Top views of α -Sb lattice structure. The unit cell is indicated by the blue rectangular box. The structure belongs to the #42 layer group $pman$. (c) STM image of α -Sb grown on SnSe substrate. (d) The height profile taken along the blue arrow in (c). (e) STM image of an α -Sb sample with 1L and 2L domains.

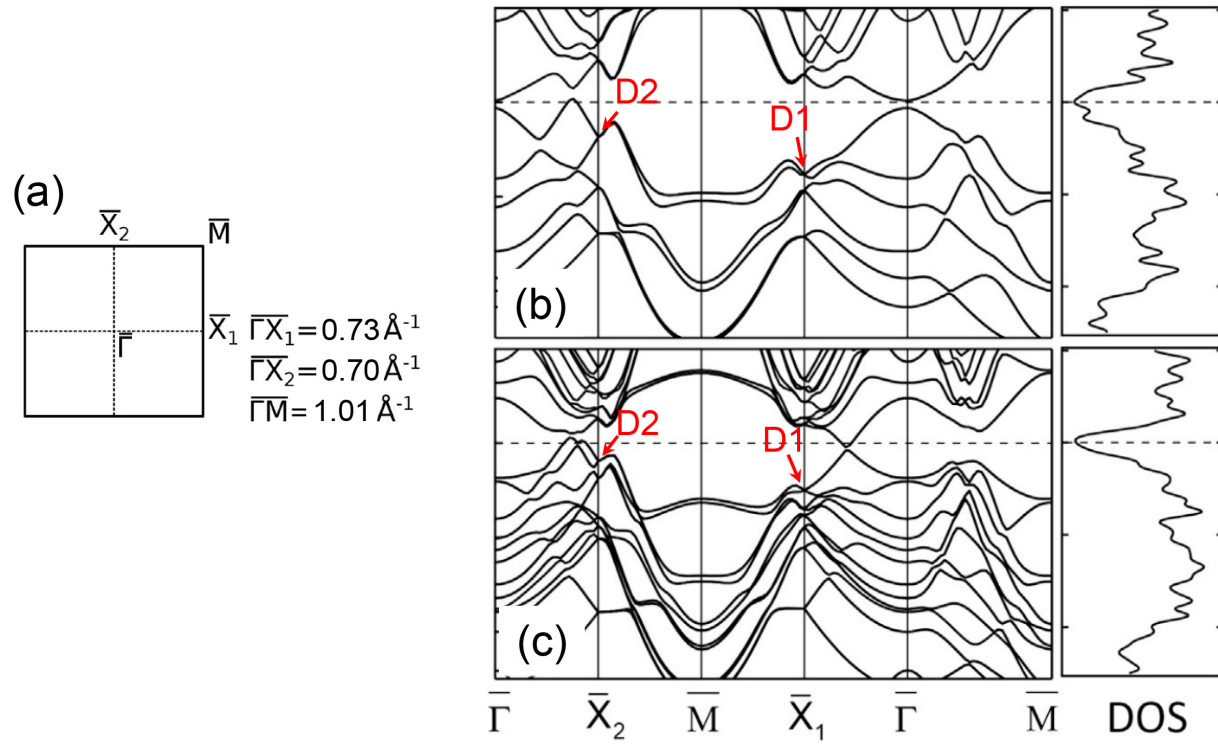


FIG. 2: (a) The Brillouin zone of α -Sb. (b) The band structure and density of states of 1L α -Sb. (c) The band structure and density of states of 2L α -Sb.

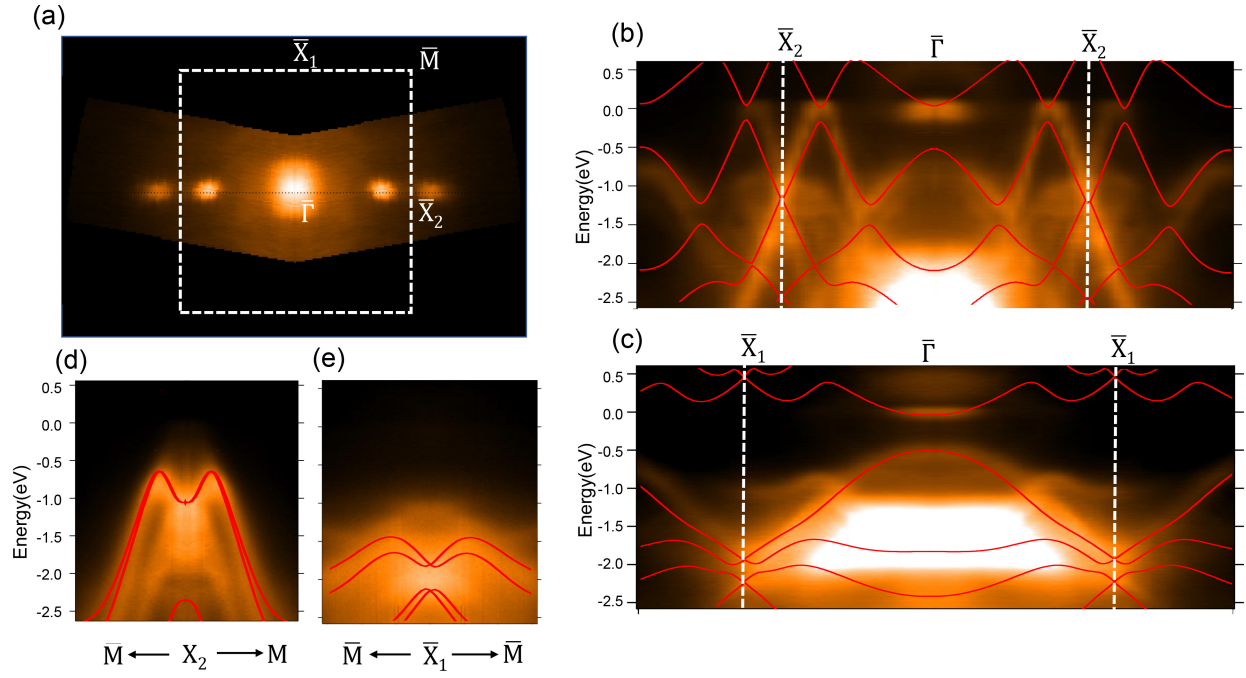


FIG. 3: (a) The Fermi surface taken from a 1L α -Sb sample by ARPES. (b, c) ARPES spectrum taken along \bar{X}_2 - $\bar{\Gamma}$ - \bar{X}_2 and \bar{X}_1 - $\bar{\Gamma}$ - \bar{X}_1 directions. (d, e) ARPES spectrum taken along \bar{M} - \bar{X}_2 - \bar{M} and \bar{M} - \bar{X}_1 - \bar{M} directions.

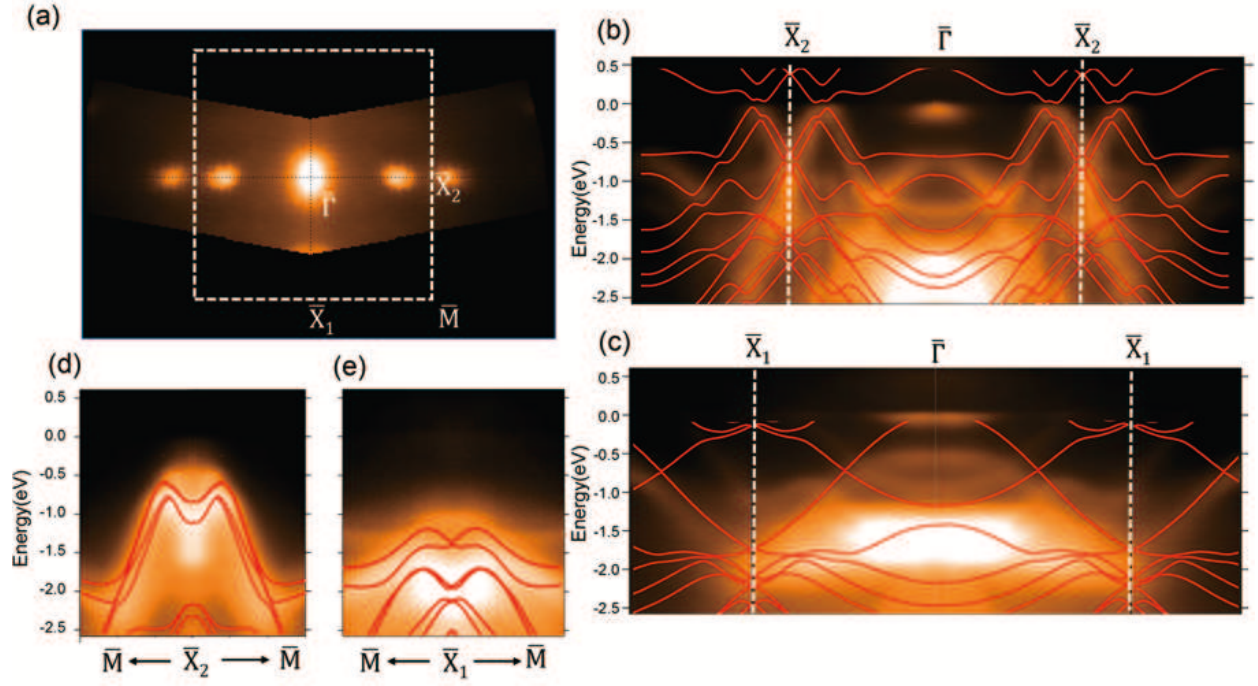


FIG. 4: (a) The Fermi surface taken from a 2L α -Sb sample by ARPES. (b, c) ARPES spectrum taken along \bar{X}_2 - $\bar{\Gamma}$ - \bar{X}_2 and \bar{X}_1 - $\bar{\Gamma}$ - \bar{X}_1 directions. (d, e) ARPES spectrum taken along \bar{M} - \bar{X}_2 - \bar{M} and \bar{M} - \bar{X}_1 - \bar{M} directions.